Published in final edited form as:
Genesis. 2010 August ; 48(8): 505–511. doi:10.1002/dvg.20639.

Zebrafish *sp7:EGFP*: a transgenic for studying otic vesicle formation, skeletogenesis, and bone regeneration

April DeLaurier, **B. Frank Eames**, **Bernardo Blanco-Sánchez**, **Gang Peng**, **Xinjun He**, **Mary E. Swartz**, **Bonnie Ullmann**, **Monte Westerfield**, and **Charles B. Kimmel**
Institute of Neuroscience, University of Oregon, Eugene, OR 97403, USA

Summary

We report the expression pattern and construction of a transgenic zebrafish line for a transcription factor involved in otic vesicle formation and skeletogenesis. The zinc finger transcription factor *sp7* (formerly called *osterix*) is reported as a marker of osteoblasts. Using bacterial artificial chromosome (BAC)-mediated transgenesis, we generated a zebrafish transgenic line for studying skeletal development, *Tg(sp7:EGFP)b1212*. Using a zebrafish BAC, *EGFP* was introduced downstream of the regulatory regions of *sp7* and injected into 1 cell-stage embryos. In this transgenic line, GFP expression reproduces endogenous *sp7* gene expression in the otic placode and vesicle, and in forming skeletal structures. GFP-positive cells were also detected in adult fish, and were found associated with regenerating fin rays post-amputation. This line provides an essential tool for the further study of zebrafish otic vesicle formation and the development and regeneration of the skeleton.

Keywords

bone; *Danio rerio*; gene transfer techniques; otic vesicle; regeneration; *sp7*

Mechanisms underlying the morphogenesis of skeletal shape are largely not understood, mainly because the ability to study the dynamic processes of cellular behavior giving rise to cartilage and bone in living embryos has been limited. In recent years, techniques have emerged that make the study of tissue formation possible *in vivo* (Beis and Stainier, 2006; Field *et al.*, 2003; Koster and Fraser, 2004), suggesting that skeletal morphogenesis can be similarly studied. The zebrafish is an ideal model organism for studying skeletal development because embryos and larvae are small and transparent, enabling the study of organogenesis in the living organism. Zebrafish cartilage and bone elements develop early and have distinct morphologies, and the genetic mechanisms underlying skeletal formation are shared with other vertebrates (Yelick and Schilling, 2002).

Transgenic lines are especially valuable for analysis of living embryos, including time-lapse confocal microscopy (Cooper *et al.*, 2005; Glickman *et al.*, 2003; Smith *et al.*, 2008). Transgenic fish lines have already been produced that express GFP in cells that give rise to, amongst other tissues, cartilage elements in the head including *Tg(−1252sox10:GFP)*^{ba5} (Dutton *et al.*, 2008) and *Tg(foxp2-enhancerA:EGFP)*^{zc42} (Bonkowsky *et al.*, 2008). A

Correspondence and requests for materials should be addressed to: April DeLaurier, Institute of Neuroscience, 1254 University of Oregon, Eugene, OR 97403 USA. april@uoneuro.uoregon.edu.
Current address of Gang Peng: Institutes of Brain Science and State Key Laboratory of Medical Neurobiology, Fudan University, Shanghai, China
Current address of Mary E. Swartz: The University of Texas at Austin, Section of Molecular Cell and Developmental Biology, College of Natural Sciences, 1 University Station C1000, Austin, Texas 78713

transgenic line expressing an observable marker of osteoblasts would help us explore osteoblast behavior specifically during the formation of intramembranous bony elements, which have no cartilaginous precursor, and for studying the induction of osteoblasts in perichondrium during endochondral ossification.

Sp7 is a zinc-finger-containing transcription factor expressed in osteoblasts and not chondrocytes, making it an excellent marker for studying osteoblasts (Nakashima *et al.*, 2002). Recently, the promoter of *sp7* has been shown to drive mCherry in osteoblasts of medaka fish allowing for the analysis of osteoblast behavior in the forming skeleton of this species (Renn and Winkler, 2009). This medaka *sp7* regulatory sequence has been used to drive fluorescent marker expression in zebrafish (Hammond and Schulte-Merker, 2009; Spoorendonk *et al.*, 2008), however, there exists no transgenic line using the regulatory region of *sp7* in zebrafish to drive a fluorescent marker in zebrafish.

We used BAC-mediated transgenesis to drive *EGFP* under the control of sequence upstream of *sp7* in a zebrafish BAC. In the case of zebrafish *sp7*, we do not know the regulatory elements necessary for gene transcription. Therefore, an advantage of using BACs for transgenesis is that they often contain large genomic clones that include the essential regulatory elements of a gene of interest. The presence of large inserts of a zebrafish-specific sequence makes it likely that the BAC contains sequence essential to drive a transgene in an expression pattern consistent with the endogenous gene. We injected the BAC into embryos to generate stable transgenic lines expressing GFP in osteoblasts. We show here the native expression pattern of *sp7* by *in situ* hybridization in whole-mounts and sections, and compare it to the expression of GFP in the *Tg(sp7:EGFP)b1212* transgenic line. We found that GFP expression reproduces endogenous *sp7* gene expression, indicating that this line will be an excellent tool for future study of the dynamic behavior of cells that create the skeleton.

sp7 expression during the formation of the otic vesicle and skeleton

Whole-mount mRNA *in situ* hybridization for *sp7* shows expression in the otic anlagen as early as 6 somite stage (~12 hours post-fertilization (hpf); Fig. 1a)(Kimmel *et al.*, 1995). Expression in the otic placode is apparent by 14 somite stage (16 hpf, Fig. 1b). By 26 hpf, otic vesicle-specific expression is significantly diminished (data not shown). *sp7* is expressed in nascent bony elements of the head by 55 hpf (Figs. 1c, d). These expression patterns match previously published results showing *in situ* expression of *sp7* mRNA in zebrafish embryos and larvae (Li *et al.*, 2009). We observe *sp7* expression in the opercle at 55 hpf (Fig. 1c). By 72 hpf, expression is also detected in the region forming the posterior branchiostegal ray (Fig. 1d). *In situ* hybridization of histological sections at 63 hpf shows expression of *sp7* in the forming opercle (Fig. 1e). Sections also reveal *sp7* expression in the perichondrium of the ceratohyal cartilage, which undergoes ossification by 96 hpf (Fig. 1f).

Generation of the *Tg(sp7:EGFP)b1212* transgenic line

A zebrafish BAC containing the *sp7* CDS (CH73-243G6) was identified using Ensembl, version 7 (http://www.ensembl.org/Danio_rerio/index.html) (Flicek *et al.*, 2008). The BAC is 89kb and contains the full *sp7* sequence, and also contains the first 3 exons of protein coding sequence for *immunoglobulin superfamily, member 8* (zgc: 77222). Since this immunoglobulin sequence is incomplete, we do not expect ectopic misexpression of a functional protein in transgenic fish, but we cannot rule this out. Purified BAC DNA was transformed into DY380 *E. coli* cells, which are engineered to allow for controlled, heat-inducible activation of recombination machinery at 42°C (Lee *et al.*, 2001). Plasmid DNA containing *EGFP* and a kanamycin *(KAN)* resistant cassette (Fig. 2a) was used as template for high-fidelity PCR. Primers were designed with arms homologous to 60 nucleotides (nt)

5’ and 3’ of the first predicted start codon of *sp7* within the BAC with 20 nt ends targeting the 5’ and 3’ ends of *EGFP* and *KAN* (see Methods). This generated a PCR product with 5’ and 3’ ends homologous to sequences 5’ and 3’ of the ATG in the BAC (Fig. 2b). *E. coli* were heat-shocked to activate recombination machinery. Homologous recombination of the PCR product into BAC DNA was assessed by PCR (Fig. 2c, see Methods). Purified BAC DNA was injected into the cytoplasm of early 1-cell stage zebrafish embryos. Founder embryos (G_0) and larvae were screened for GFP expression between 24 hpf and 6 days post-fertilization (dpf). GFP-expressing fish were out-crossed to wild-type (ABC) fish at 8 weeks of age and G_1 progeny were screened. Germline transmission of BACs may occur in 2–3% of injected fish (Yang *et al.*, 2006). Identical GFP expression patterns were detected in several transient transgenic fish and in two G_1 fish that became founders for stable lines. There is no observable phenotype in homozygous transgenic fish.

Characterization of GFP expression in the *Tg(sp7:EGFP)b1212* line

Early expression of GFP is detected at 6 somite stage embryos, in the otic anlagen (Fig. 3a). At 14 somites, GFP expression is strongly detected in the otic placode (Fig. 3b). Expression remains in the otic vesicle beyond 24 hpf, and also in the statoacoustic ganglion anterior to the ventral aspect of the otic vesicle (Figs. 3c, d). Beyond 48 hpf, expression in the ear becomes fainter, but does not disappear entirely (data not shown). By 3 dpf, expression in cells associated with developing bone, e.g., the opercle, is detected along with Alizarin red, which stains mineralized matrix (Fig. 3f). By 96 hpf (4 dpf), GFP-positive cells associated with the posterior branchiostegal ray are detected (Figs. 3g, h). At 4dfp, we observe that the opercle has expanded ventrally to form a “fan-like” shape (Fig. 3h, (Li *et al.*, 2009)). Throughout development of the opercle and posterior branchiostegal ray (Figs. 3j, l), GFP is predominantly expressed in cells at the ventral edge of the element. GFP-positive cells, however, are still associated within the region of mineralized matrix, and are present surrounding all edges of the element. Expression of GFP is detected in cells surrounding the mineralized portion of the ceratohyal at 150 hpf (but not prior to this stage, see Figs. 3e, g), immediately adjacent to Alizarin red-positive matrix, demonstrating osteoblasts secreting perichondral bone (Figs. 3i, k). At 17dpf (Fig. 3m), GFP is detected in cells surrounding the growing edges of bony elements, in patterns that sometimes appear element-specific (Fig. 3m). GFP was not detected in chondrocytes forming elements of the second pharyngeal arch at any stage examined (i.e., hyomandibular and ceratohyal cartilages), although expression was detected in chondrocytes of the first arch Meckel’s cartilage (data not shown). GFP in chondrocytes of the Meckel’s cartilage has been previously observed by Hammond and Shulte-Merker (2009) using a medaka *sp7* transgenic reporter line. Based on figures 3a–h, GFP expression reproduces mRNA expression of *sp7* (Fig. 1c and d).

In adult transgenic zebrafish, GFP-positive cells are detected associated with skeletal elements, such as the tail fin bony rays (Fig. 3o). When rays are amputated, GFP-positive cells, putative osteoblasts, are detected associated with the site of amputation 2 days post-amputation (dpa), increasing in number by 3 dpa, and associated with the formation of newly mineralized matrix regenerating ray bone by 5 dpa (Figs. 3p–s). The presence of GFP-positive cells at the site of amputation is supported by *in situ* analyses showing expression of *sp7* mRNA associated with regenerating fin rays at 5 dpa (Brown *et al.*, 2009).

Significance of transgenic lines

Expression of *sp7* in the otic primordium has been reported in embryos as early as 1 somite stage (Thisse and Thisse, 2005), although the function of Sp7 in otic vesicle formation has not been established. This line labels the otic anlagen before the otic placode becomes morphologically visible in a live embryo. Thus, this line provides a tool for the processes

that regulate otic competence, induction and specification, including placodal transplants or rotation experiments, as well for studies of stato-acoustic ganglion development. Transgene expression in skeletogenic tissues appears similar to that described using the medaka *sp7* promoter driving fluorescent transgene expression in zebrafish (Hammond and Schulte-Merker, 2009), although otic vesicle expression has not been previously described.

This line has great potential for studying the formation of dermal bones and ossification of cartilage during development, and during regeneration of skeletal elements. Future studies could include dynamic analysis of changing bone shape during development (Kimmel *et al.*, 2010), analysis of mutants that have altered dermal bone shape such as the *mef2ca* mutant (Miller *et al.*, 2007), and analysis of genetic pathways and mechanisms of skeletal repair in response to injury.

Methods

Cloning of *sp7*

Zebrafish *sp7* has been sequenced and annotated in ensembl (http://www.ensembl.org/Danio_rerio/index.html), where the gene is identified as ENSDARG00000019516 (Flicek *et al.*, 2008).

Whole-mount and section mRNA *in situ* hybridization

To make probes for expression analysis, a 576 bp segment of *sp7* gene was cloned from 1 dpf zebrafish whole embryo cDNA with primers: F: 5'-GAAGTCCTCCACCGGCTCCAACA and R: 5'-TCGGGCAATCGCAAGAAGACCT. PCR product was inserted into pCR4 TOPO vector (Invitrogen, Eugene, OR). *sp7* plasmid was cut with *Not*I and RNA was synthesized with T3 RNA polymerase. Whole-mount *in situ* hybridization was performed as described (Miller *et al.*, 2000; Westerfield, 2007; Yokoi *et al.*, 2009). Section *in situ* hybridization to tissue sections was performed as described (Rodriguez-Mari *et al.*, 2005).

Selection of BAC clone

The *sp7* BAC clone was ordered from the Children's Hospital Oakland Research Institute (CHORI) BACPAC Resources Center (BPRC). The presence of *sp7* was confirmed by PCR with primers: F: 5'-TCGCTCAATCCTCAAATGCC and R: 5'-TGTCAATCGCTGTCAAACCACTG.

Transformation of BAC clone into DY380 cells

Transformation of cells followed a modified version of a published protocol (Warming *et al.*, 2005) as follows: DY380 cells (National Cancer Institute, Frederick, MD; now available as SW102 strain) were prepared for electroporation-competent cells in 50μl of 10% glycerol. 5μl of purified BAC DNA was added to the cells, which were electroporated at 2.5kV (single pulse, Biorad E. coli Pulser). Cells were plated on LB-CAM agar plates for selection of BAC-containing colonies.

Generation of transgenic construct

Oligonucleotide primers were designed with arms homologous to 60 nt 5' or 3' of the ATG of the gene of interest within the BAC with 20 nt ends targeting the 5' or 3' ends of a plasmid containing *EGFP-flpe-KAN* (*EGFP* sequence underlined; F: 5'-AACACTGCAATTACTCTTTAAATCTCTTCTCAGGAGGAAACACGTTATGGATCC AGT CCCATGGTGAGCAAGGGCGAGG, R: 5'-TTTTAATAGGGATGGTGCTTCCCGGTTTACCAGGTGTGGCAGAATCTCGGACTG

GACTGGCTATTCCAGAAGTAGTGAGGAG). Primers were designed to induce a frame-shift in the coding sequence of the first exon of *sp7* to avoid ectopic over-expression of Sp7. High-fidelity PCR was performed using the *EGFP-flpe-KAN* DNA as template to produce a product to be used for homologous recombination with the BAC DNA. PCR conditions were as follows: (Phusion, Finnzymes, Espoo, Finland) 98°C, 30 sec, 98°C, 10sec, 74°C, 30 sec, 72°C, 1min 30 sec for 35 cycles, then 72°C for 10 min. PCR product was purified using ZYMO DNA purification columns (Zymo Research, Orange, CA), and digested with *Dpn*I (New England Biolabs, Ipswich, MA), resolved on an agarose gel and the band was purified (Qiagen Gel Extraction kit, Qiagen). DNA was eluted with 25μl buffer EB diluted 1:5 in distilled H_2O.

Heat-shock and homologous recombination

A single DY380 colony containing BAC DNA was grown overnight and prepared for electroporation-competent cells as described (Lee *et al.*, 2001; Warming *et al.*, 2005). 10μl of purified PCR product was transformed into cells by electroporation. Transformed cells were recovered in SOC media and plated onto LB-CAM-KAN agar plates for double selection of both the BAC (CAM) and the PCR product (KAN).

Purification and injection of construct

Colony PCR was performed to verify the homologous recombination of the *EGFP-KAN* DNA with BAC overhangs into the BAC plasmid using two pairs of primer sets designed at 5' of the ATG (F: 5'-CGCAATGCCTCAAAACCACTC, R: 5'-AACTTCAGGGTCAGCTTGCCGTAG) and 3' of the ATG (F: 5'-CGTGATATTGCTGAAGAGCTTGG, R: 5'-TGGAGGACTTCCAGTTGGTGTTAG). Homologous insertion of the transgene and a frame-shift in the *sp7* coding sequence in the BAC was confirmed by sequence analysis (Fig. 2). Bacterial cultures were purified according to the manufacturer's protocol (Nucleobond PC 20, Clontech Laboratories, Inc., Mountain View, CA) and BAC DNA was recovered with 25μl of pre-warmed buffer 1/5 EB. DNA was injected in a concentration of 30 ng/μl with 2% phenol red. Approximately 3 nl was injected directly into the cytoplasm of early 1-cell stage zebrafish embryos. The ABC Oregon wild-type stock was used for injection and later out-crosses. Embryos were maintained under standard conditions (Westerfield, 2007) and staged as described (Kimmel *et al.*, 1995). The University of Oregon Institutional Animal Care and Use Committee approved all work with vertebrate animals.

Alizarin red staining and imaging

Live fish were stained using the vital dye, Alizarin red, which labels mineralized matrix (Walker and Kimmel, 2007), and fluoresces in the red spectrum. Larvae and adult fish were incubated in 30ml embryo medium or fish water with 200μl 0.5% Alizarin red (Sigma, St. Louis, MO) dissolved in H_2O for 2–3hrs, rinsed in plain embryo medium or fish water, then imaged on a confocal microscope detecting both the transgene (488nm laser) and the Alizarin stain (543nm laser) (Zeiss, LSM 5 Pascal, Thornwood, NY).

Tail fin amputation

The caudal fins of adult homozygous transgenic fish were amputated under anesthetic (Westerfield, 2007). The tails of anesthetized, living fish were confocal imaged on days 1, 2, 3, and 5 dpa. On day 5 pa, live fish were stained with Alizarin Red as described above, prior to imaging.

Acknowledgments

We thank Y. Honjo, J. Postlethwait and H. Yokoi for input and manuscript revisions, J. Dowd, J. Pierce, and the University of Oregon Zebrafish Facility for providing animals and excellent fish care. Undergraduate assistance was provided by S. Kamenko. Section *in situ* hybridizations were performed by R. BreMiller and Y. Yan. We are grateful to the University of Oregon zebrafish 'groupie' attendees for helpful and friendly input.

Contract grant sponsors: NIH, NIDCD, NIHCR.

References

Beis D, Stainier DY. In vivo cell biology: following the zebrafish trend. Trends Cell Biol. 2006; 16:105–112. [PubMed: 16406520]

Bonkowsky JL, Wang X, Fujimoto E, Lee JE, Chien CB, Dorsky RI. Domain-specific regulation of foxP2 CNS expression by lef1. BMC Dev Biol. 2008; 8:103. [PubMed: 18950487]

Brown AM, Fisher S, Iovine MK. Osteoblast maturation occurs in overlapping proximal-distal compartments during fin regeneration in zebrafish. Dev Dyn. 2009; 238:2922–2928. [PubMed: 19842180]

Cooper MS, Szeto DP, Sommers-Herivel G, Topczewski J, Solnica-Krezel L, Kang HC, Johnson I, Kimelman D. Visualizing morphogenesis in transgenic zebrafish embryos using BODIPY TR methyl ester dye as a vital counterstain for GFP. Dev Dyn. 2005; 232:359–368. [PubMed: 15614774]

Dutton JR, Antonellis A, Carney TJ, Rodrigues FS, Pavan WJ, Ward A, Kelsh RN. An evolutionarily conserved intronic region controls the spatiotemporal expression of the transcription factor Sox10. BMC Dev Biol. 2008; 8:105. [PubMed: 18950534]

Field HA, Ober EA, Roeser T, Stainier DY. Formation of the digestive system in zebrafish. I. Liver morphogenesis. Dev Biol. 2003; 253:279–290. [PubMed: 12645931]

Flicek P, Aken BL, Beal K, Ballester B, Caccamo M, Chen Y, Clarke L, Coates G, Cunningham F, Cutts T, Down T, Dyer SC, Eyre T, Fitzgerald S, Fernandez-Banet J, Graf S, Haider S, Hammond M, Holland R, Howe KL, Howe K, Johnson N, Jenkinson A, Kahari A, Keefe D, Kokocinski F, Kulesha E, Lawson D, Longden I, Megy K, Meidl P, Overduin B, Parker A, Pritchard B, Prlic A, Rice S, Rios D, Schuster M, Sealy I, Slater G, Smedley D, Spudich G, Trevanion S, Vilella AJ, Vogel J, White S, Wood M, Birney E, Cox T, Curwen V, Durbin R, Fernandez-Suarez XM, Herrero J, Hubbard TJ, Kasprzyk A, Proctor G, Smith J, Ureta-Vidal A, Searle S. Ensembl 2008. Nucleic Acids Res. 2008; 36:D707–D714. [PubMed: 18000006]

Glickman NS, Kimmel CB, Jones MA, Adams RJ. Shaping the zebrafish notochord. Development. 2003; 130:873–887. [PubMed: 12538515]

Hammond CL, Schulte-Merker S. Two populations of endochondral osteoblasts with differential sensitivity to Hedgehog signalling. Development. 2009; 136:3991–4000. [PubMed: 19906866]

Kimmel CB, Ballard WW, Kimmel SR, Ullmann B, Schilling TF. Stages of embryonic development of the zebrafish. Dev Dyn. 1995; 203:253–310. [PubMed: 8589427]

Kimmel CB, DeLaurier A, Ullmann B, Dowd J, McFadden M. Modes of developmental outgrowth and shaping of a craniofacial bone in zebrafish. PLoS One. 2010; 5:e9475. [PubMed: 20221441]

Koster RW, Fraser SE. Time-lapse microscopy of brain development. Methods Cell Biol. 2004; 76:207–235. [PubMed: 15602878]

Lee EC, Yu D, Martinez de Velasco J, Tessarollo L, Swing DA, Court DL, Jenkins NA, Copeland NG. A highly efficient Escherichia coli-based chromosome engineering system adapted for recombinogenic targeting and subcloning of BAC DNA. Genomics. 2001; 73:56–65. [PubMed: 11352566]

Li N, Felber K, Elks P, Croucher P, Roehl HH. Tracking gene expression during zebrafish osteoblast differentiation. Dev Dyn. 2009; 238:459–466. [PubMed: 19161246]

Miller CT, Schilling TF, Lee K, Parker J, Kimmel CB. sucker encodes a zebrafish Endothelin-1 required for ventral pharyngeal arch development. Development. 2000; 127:3815–3828. [PubMed: 10934026]

Miller CT, Swartz ME, Khuu PA, Walker MB, Eberhart JK, Kimmel CB. mef2ca is required in cranial neural crest to effect Endothelin1 signaling in zebrafish. Dev Biol. 2007; 308:144–157. [PubMed: 17574232]

Nakashima K, Zhou X, Kunkel G, Zhang Z, Deng JM, Behringer RR, de Crombrugghe B. The novel zinc finger-containing transcription factor osterix is required for osteoblast differentiation and bone formation. Cell. 2002; 108:17–29. [PubMed: 11792318]

Renn J, Winkler C. Osterix-mCherry transgenic medaka for in vivo imaging of bone formation. Dev Dyn. 2009; 238:241–248. [PubMed: 19097055]

Rodriguez-Mari A, Yan YL, Bremiller RA, Wilson C, Canestro C, Postlethwait JH. Characterization and expression pattern of zebrafish Anti-Mullerian hormone (Amh) relative to sox9a, sox9b, and cyp19a1a, during gonad development. Gene Expr Patterns. 2005; 5:655–667. [PubMed: 15939378]

Smith KA, Chocron S, von der Hardt S, de Pater E, Soufan A, Bussmann J, Schulte-Merker S, Hammerschmidt M, Bakkers J. Rotation and asymmetric development of the zebrafish heart requires directed migration of cardiac progenitor cells. Dev Cell. 2008; 14:287–297. [PubMed: 18267096]

Spoorendonk KM, Peterson-Maduro J, Renn J, Trowe T, Kranenbarg S, Winkler C, Schulte-Merker S. Retinoic acid and Cyp26b1 are critical regulators of osteogenesis in the axial skeleton. Development. 2008; 135:3765–3774. [PubMed: 18927155]

Thisse C, Thisse B. High Throughput Expression Analysis of ZF-Models Consortium Clones. ZFIN Direct Data Submission. 2005

Walker MB, Kimmel CB. A two-color acid-free cartilage and bone stain for zebrafish larvae. Biotech Histochem. 2007; 82:23–28. [PubMed: 17510811]

Warming S, Costantino N, Court DL, Jenkins NA, Copeland NG. Simple and highly efficient BAC recombineering using galK selection. Nucleic Acids Res. 2005; 33:e36. [PubMed: 15731329]

Westerfield, M. The Zebrafish Book: A Guide for the Laboratory Use of Zebrafish (Brachydanio Rerio). 5th ed.. Eugene: University of Oregon Press; 2007.

Yang Z, Jiang H, Chachainasakul T, Gong S, Yang XW, Heintz N, Lin S. Modified bacterial artificial chromosomes for zebrafish transgenesis. Methods. 2006; 39:183–188. [PubMed: 16828309]

Yelick PC, Schilling TF. Molecular dissection of craniofacial development using zebrafish. Crit Rev Oral Biol Med. 2002; 13:308–322. [PubMed: 12191958]

Yokoi H, Yan YL, Miller MR, BreMiller RA, Catchen JM, Johnson EA, Postlethwait JH. Expression profiling of zebrafish sox9 mutants reveals that Sox9 is required for retinal differentiation. Dev Biol. 2009; 329:1–15. [PubMed: 19210963]

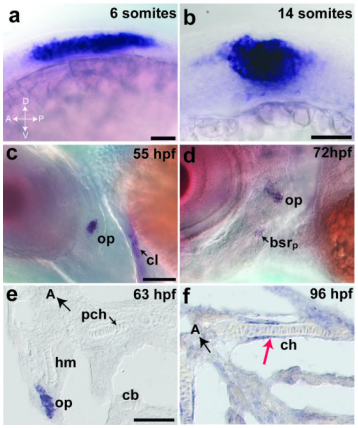

Fig. 1.

Whole-mount and section mRNA *in situ* hybridization to detect expression of *sp7*. a–d are whole-mount lateral views of the zebrafish head region (A = anterior, P = posterior, D = dorsal, V = ventral). e is a transverse section and f is a horizontal section through the head (A = anterior). a and b: *sp7* is expressed in the developing otic anlagen (a) and otic placode (b). c and d: *sp7* is expressed in the developing op and posterior bsr of the zebrafish craniofacial skeleton. e: *sp7* is expressed cells of the op. f: *sp7* is expressed in cells of the perichondrium surrounding the ch cartilage, associated with ossification of this element (indicated by arrow). Abbreviations: bsr_p = posterior branchiostegal ray, cb = ceratobranchial, ch = ceratohyal, cl = cleithrum, hm = hyomandibular, op = opercle, pch = parachordal. Scale bars: a = 50μm, b = 100μm, c and d = 200μm, e and f = 100μm.

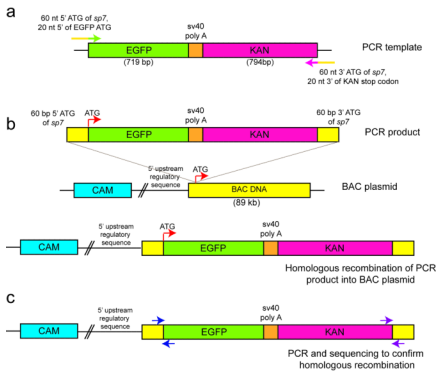

Fig. 2.

BAC-mediated transgenesis procedure. a: An *EGFP-KAN* (kanamycin) construct is used as template DNA for PCR to generate a product for recombination with BAC DNA. Primers are designed with homologous arms 60 nt 5' (forward) or 3' (reverse) of the ATG of *sp7* (see Methods). b: Homologous recombination of the PCR product into the ATG locus of *sp7* in BAC DNA with *CAM* (chloramphenicol) resistance. Recombined plasmid contains 5' upstream regulatory sequence of the gene of interest driving the *EGFP* transgene. Expression of the BAC DNA does not result in overexpression of the gene of interest as transgene insertion replaces the native ATG of the gene. c: PCR is performed to verify the homologous recombination of the *EGFP-KAN* DNA with BAC overhangs into the BAC plasmid 5' of the ATG of *EGFP-KAN* DNA (blue arrows) and 3' of the ATG of *sp7* DNA (purple arrows).

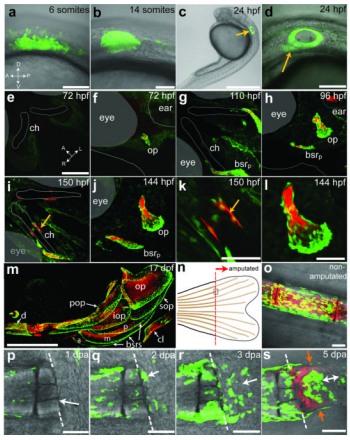

Fig. 3.

Expression of GFP in the *Tg(sp7:EGFP)b1212* transgenic line in living zebrafish embryos, larvae, and adults. Samples in panels e–o and s are stained with vital Alizarin red to label mineralized matrix. a–d, f, h, j, l, m, and o–s are lateral views (A = anterior, P = posterior, D = dorsal, V = ventral) and e, g, i, and k are ventral views (A = anterior, L = left, R = right). All panels are projections of confocal z-stacks, except figs. b, c and d, which are single z-sections. a and b: GFP is expressed in the otic anlagen and otic placode, respectively. c and d: GFP is expressed in the otic vesicle, and in the statoacoustic ganglion anterior to the otic vesicle (indicated by arrows). e and f: No GFP expression is detected in cartilaginous elements (i.e. ch), but GFP is expressed in cells forming the op. g and h: GFP is strongly expressed in cells of the bsr_p and the op, but is not associated with the ch. i–l (k and l are high-magnification images of i and j, respectively): GFP is expressed in osteoblasts of the growing op and bsr_p, and also in perichondral osteoblasts of the ch (indicated by arrows in i and k). m: At larval stages, GFP expression is present in growing bones of the jaw and jaw supporting structure. n: schematic showing location of amputation of adult tail fin. o: non-amputated adult fin ray showing GFP-positive cells associated with mineralized matrix. p–s: time series of GFP-positive cell association with the site of amputation (indicated by dotted line) between 1–5 dpa (indicated by white arrows). At 5 dpa, GFP-positive cells are also detected in forming ray bone away from the site of amputation (indicated by white double arrow). Orange arrows indicate the extent of new bone growth at 5 dpa. Compared with the unamputated control (Fig. 3o), uncut bone adjacent to the amputated site does not stain with Alizarin Red. The reason for this remains unclear and requires further investigation. After 72hpf, green fluorescence is detected in the skin of fish (not shown). This does not interfere with confocal imaging of skeletal structures of fish at any stage, because bones are below the plane of focus of the skin. Abbreviations: bsr = branchiostegal rays, where bsr_a = anterior, bsr_m = middle, bsr_p = posterior, ch = ceratohyal, cl = cleithrum, d = dentary, iop = interopercle, op = opercle, pop = preopercle, sop = subopercle. Scale bars: a = 100μm, b = 50μm, c = 500μm, d = 100μm, e–j = 100μm, k and l = 50μm, m = 500μm, o–s = 50μm.